Bioorganic Chemistry 44 (2012) 8–18

Contents lists available at SciVerse ScienceDirect

Bioorganic Chemistry

journal homepage: www.elsevier.com/locate/bioorg

Evaluation of the association of mercury(II) with some dicysteinyl tripeptides

Xiuli Lin [a], Jeremy Brooks [b], Matthew Bronson [b], Maria Ngu-Schwemlein [b,*]

[a] Department of Chemistry, Wake Forest University, Winston-Salem, NC 27109, USA
[b] Department of Chemistry, Winston-Salem State University, Winston-Salem, NC 27110, USA

ARTICLE INFO

Article history:
Received 24 January 2012
Available online 23 June 2012

Keywords:
Cysteinyl peptides
Mercury(II) binding
Isothermal titration calorimetry
Thermodynamic parameters
Orbitrap ESI mass spectrometry
Mercury(II) and cysteinyl complexes
Binding enthalpy
Stability constants

ABSTRACT

The present study was undertaken to gain insight into the associations of mercury(II) with dicysteinyl tripeptides in buffered media at pH 7.4. We investigated the effects of increasing the distance between cysteinyl residues on mercury(II) associations and complex formations. The peptide–mercury(II) formation constants and their associated thermodynamic parameters in 3-(*N*-morpholino)propanesulfonic acid (MOPS) buffered solutions were evaluated by isothermal titration calorimetry. Complexes formed in different relative ratios of mercury(II) to cysteinyl peptides in ammonium formate buffered solutions were characterized by LTQ Orbitrap mass spectrometry. The results from these studies show that *n*-alkyl dicysteinyl peptides (**CP 1–4**), and an aryl dicysteinyl peptide (**CP 5**) can serve as effective "double anchors" to accommodate the coordination sites of mercury(II) to form predominantly one-to-one Hg(peptide) complexes. The aryl dicysteinyl peptide (**CP 5**) also forms the two-to-two $Hg_2(peptide)_2$ complex. In the presence of excess peptide, $Hg(peptide)_2$ complexes are also detected. Notably, increasing the distance between the ligating groups or "anchor points" in **CP 1–5** does not significantly affect their affinity for mercury(II). However, the enthalpy change (ΔH) values ($\Delta H_1 \sim -91$ kJ mol^{-1} and $\Delta H_2 \sim -66$ kJ mol^{-1}) for complex formation between **CP 4** and **5** with mercury(II) are about one and a half times larger than the related values for **CP 1**, **2** and **3** ($\Delta H_1 \sim -66$ kJ mol^{-1} and $\Delta H_2 \sim 46$ kJ mol^{-1}). The corresponding entropy change (ΔS) values ($\Delta S_1 \sim -129$ J K^{-1} mol^{-1} and $\Delta S_2 \sim -116$ J K^{-1} mol^{-1}) of the structurally larger dicysteinyl peptides **CP 4** and **5** are less entropically favorable than for **CP 1**, **2** and **3** ($\Delta S_1 \sim -48$ J K^{-1} mol^{-1} and $\Delta S_2 \sim -44$ J K^{-1} mol^{-1}). Generally, these associations result in a decrease in entropy, indicating that these peptide–mercury complexes potentially form highly ordered structures. The results from this study show that dicysteinyl tripeptides are effective in binding mercury(II) and they are promising motifs for the design of multi-cysteinyl peptides for binding more than one mercury(II) ion per peptide.

© 2012 Elsevier Inc. All rights reserved.

1. Introduction

Mercury is a toxic element that can exist in several physical and chemical forms [1]. Once mercury is released into the atmosphere, it is persistent and readily becomes a bioaccumulative toxic pollutant by making its way up the food chain [2]. All forms of mercury are toxic and exposure to them can be detrimental to the brain, kidney, and lungs, resulting in neurotoxicity, hepatotoxicity, nephrotoxicity, or pulmonary toxicity [3,4]. Current clinical chelation therapy of mercury poisoning [5] generally uses thiol compounds such as dimercaptosuccinic acid (DMSA), dimercaptopropanesulfonic acid (DMPS), and when necessary, cysteine (Cys) and N-acetylcysteine (NAC) for hemodialysis [6,7]. However, it has been shown that these are not well-optimized molecules for mercury chelation therapy [8,9]. Therefore it is useful to study other options for the therapeutic chelation of mercury.

The thiol group of cysteine residue plays an important role as a donor atom for metal ion coordination in metalloproteins and metallopeptides. For example, the tripeptide glutathione (GSH, γ-Glu-Cys-Gly) is a peptide thiol found in plants and animals [10]. One of its many biochemical functions is its role in protecting plants and animals from cellular damage arising from heavy metal ions such as mercury, lead, and cadmium. Other thiol-rich peptides include metallothioneins and phytochelatins; both of which consist of a two-cysteine residue motif, which plays a crucial role in binding and sequestering heavy metal ions [11,12].

The distinct "soft acid" character of the mercury(II) ion shows a strong binding affinity for ligands with "soft base" donor atoms such as sulfur, selenium and phosphorus. This is in agreement with Pearson's principles [13], and accordingly, the cysteinyl thiol group and mercury(II) form stable complexes. Indeed, thiolates have been traditionally referred to as mercaptans because of their tendency to capture mercury [14]. Mercury(II) (d^{10}) often forms complexes with low coordination numbers, and frequently with a preference for a linear two-coordinate complex [15a]. However, they may also

* Corresponding author. Fax: +1 336 750 2549.
E-mail address: Schwemleinmn@wssu.edu (M. Ngu-Schwemlein).

0045-2068/$ - see front matter © 2012 Elsevier Inc. All rights reserved.
http://dx.doi.org/10.1016/j.bioorg.2012.06.001

react with additional ligands to form higher-coordinate trigonal planar or tetrahedral complexes [15a].

Cysteinyl peptide ligands have a number of potential coordinating sites in addition to the thiol group. The involvement of the amide nitrogen, carbonyl oxygen, N-terminal amino, C-terminal carboxyl groups, and their side chain functionalities depend on the steric constraints on the complex or chelate formed. However, the thiol group in cysteinyl peptides will be the primary ligating group or "anchor" to mercury(II) in the formation of a stable peptide–mercury(II) complex because of their preferential soft S-donor and soft Hg–acceptor interactions. Accordingly, peptides containing two cysteine residues that are optimally spaced could serve as "double anchors" to mercury(II) by forming a linear two-coordinate complex. Additionally, peptides containing multiple dicysteinyl motifs could enhance the binding efficiency by ligating more than one mercury(II) per peptide or by forming higher coordination complexes. Moreover, these peptides would form structurally larger mercury–peptide complexes that could better evade transport into brain cells via amino acid transporters by molecular mimicry [16,17]. Structurally small mercury–cysteine complexes have been shown to enter cells through amino acid transporters by molecular mimicry. For example, Bridges and Zalups showed that cysteine S-conjugates of inorganic mercury and the amino acid cystine are both transported by the same amino acid transport system whereby the complex acts as a structural and/or functional homologue of cystine [17,18].

Recently, we reported the thermodynamic parameters of the interactions of mercury(II) with some di- and tri-peptides of cysteine containing histidine, for its imidazole-*N*-donor atom, and tryptophan, for its potential electrostatic cation-pi interactions [19]. Isothermal titration calorimetric studies showed that these thiol S-donor peptides exhibit two binding enthalpies for mercury(II). Their stability constants for the first binding (10^8 to $>10^{10}$ M^{-1}) are largely due to favorable contribution of the enthalpy term to the free energy of complexation. In the second association, the enthalpy contribution decreases and the free energy of the second binding (10^5–10^6 M^{-1}) is partly compensated by the entropy term. As the monothiol S-donor peptide ligand increases in size, from di- to tri-peptides, the binding constant decreases as the contribution of the enthalpy term to the free energy of complexation decreases. However, binding can be improved by increasing the number of thiol S-donor groups in the tripeptide as demonstrated by the dithiol peptide Cys-Trp-Cys [19].

The present study was undertaken to better understand the interactions of dicysteinyl tripeptides with mercury(II) by evaluating the binding properties of *n*-alkyl dicysteinyl peptides (**CP 1–4**), and an aryl dicysteinyl peptide (**CP 5**) (Fig. 1) with mercury(II). The effects of increasing the distance and linker type between cysteinyl residues were evaluated. We report here the thermodynamic parameters, enthalpy (ΔH), entropy (ΔS), and free energy (ΔG), including the binding constant (K_b), for the interactions between these cysteinyl peptides and mercury(II) in 3-(*N*-morpholino)propanesulfonic acid (MOPS) buffered solutions at pH 7.4 by isothermal titration microcalorimetry (ITC). Additionally, the complexes formed by direct reaction of mercury(II) ions and cysteinyl peptides, in ammonium formate buffered solutions containing different relative ratios of mercury(II) to peptide, were also characterized by LTQ Orbitrap mass spectrometry.

2. Experimental

2.1. Materials and methods

All chemicals were obtained from commercial suppliers and used without further purification. Fmoc-Cys(Trt)(Wang Resin LL)-resin, 1-hydroxy-7-azabenzotriazole (HOAT), O-(7-azabenzotriazol-1-yl)-N,N,N′,N′-tetramethyluronium hexafluorophosphate (HATU), ethyl cyano(hydroxyimino)acetate (Oxyma Pure), Fmoc-Gly(Dmb)-OH, Fmoc-Gly-OH, and Fmoc-Cys(Trt)-OH were purchased from EMD Chemicals, Inc. (San Diego, California, USA). Collidine (TMP), triisopropylsilane (TIS), 3,6-dioxa-1,8-octanedithiol (DODT), trifluoroacetic acid (TFA), diisopropylcarbodiimide (DIPCDI), and dichloromethane (DCM), were obtained from Sigma–Aldrich (St. Louis, Missouri, USA). Fmoc-aminomethylphenyl acetic acid was purchased from AnaSpec, Inc. (Fremont, California, USA). N,N-dimethylformamide (DMF) and anhydrous ether were obtained from VWR (Westchester, PA). HPLC grade water and HPLC grade acetonitrile were purchased from Fisher Scientific (Pittsburgh, Pennsylvania, USA). Reversed-phase C-18 HPLC columns (Gemini) were purchased from Phenomenex, Inc. (Torrance, California, USA).

Mercury(II) nitrate (>98%), was purchased from Sigma–Aldrich (Milwaukee, USA). The series of *n*-alkyl di-cysteinyl peptides (**CP 1–4**) (>95% purity) were purchased from New England Peptide (Massachusetts, USA). **CP 5** (>95%) was prepared by microwave-assisted solid phase peptide synthesis, as described below.

2.2. Preparation of CP 5

CP 5 was prepared by microwave-assisted solid phase peptide synthesis following the standard Fmoc-strategy by using a CEM Discovery microwave peptide synthesizer (CEM, Corp., Matthews, North Carolina, USA). Fmoc-Cys(Trt)(Wang Resin LL)-resin (0.5 meq/g substitution, 0.2 g, 0.1 mmol) was loaded onto a 25 mL polypropylene reaction tube fitted with a fiber-optic temperature probe for controlling the microwave power, polyethylene filter and a Teflon™ seal ball. Deprotections were performed with 20% piperidine and 0.1 M Oxyma Pure in DMF solution with a deprotection of 4 min at 22 W with a maximum temperature of 75 °C. The coupling with a 5-fold molar excess of Fmoc-aminomethylphenyl acetic dissolved in HATU:collidine:amino acid (0.9:2:1 mol equivalence) in DMF was performed twice. These reactions were conducted under microwave irradiation at 25 W for 6 min with a maximum temperature of 75 °C. The coupling reaction condition for cysteine was altered to 1 h at room

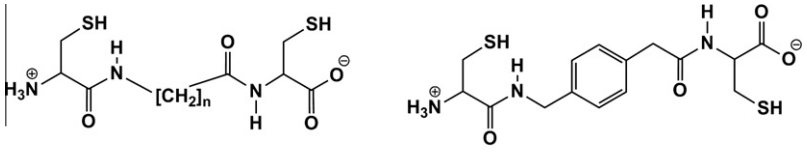

Cysteinyl tripeptides
CP 1 (n = 1); **CP 2** (n = 2)
CP 3 (n = 3); **CP 4** (n = 4)

Cysteinyl tripeptide **CP 5**

Fig. 1. Chemical structures of **CP 1–5** dicysteinyl tripeptides.

temperature. After Fmoc deprotection, the tripeptide resin was then washed successively with dimethylformamide (3 × 5 mL), dichloromethane (3 × 5 mL), methanol (1 mL), and dried overnight under high vacuum. Final cleavage from the resin and deprotection of the amino acid side chain protecting groups were carried out with a solution of TFA/H_2O/TIS/DODT (92.5%, 2.5%, 2.5%, and 2.5%, respectively) (6 mL) at 19 W for 1 h with a maximum temperature of 38 °C. Following cleavage, the peptide was precipitated with 40 mL of ice-cold anhydrous ether, centrifuged, washed three times with 40 mL cold ether, and dried under high vacuum overnight. Analytical HPLC of crude peptides was performed using a C-18 reversed-phase Gemini column (110 Å, 5 μm, 4.6 mm × 250 mm), whereas HPLC purification was conducted with a semi-preparative C-18 reversed-phase Gemini column (110 Å, 5 μm, 10 mm × 250 mm). The mobile phase was H_2O/0.1% trifluoroacetic acid (TFA) (A), and acetonitrile/0.08% TFA (B), delivered by a Rainin Dynamax 300 HPLC system with UV monitoring at 220 nm. Analytical HPLC employed 5% B to 30% B over 30 min with a flow rate of 1 mL/min. The retention time for **CP 5** is 16.3 min. Following purification by semi-preparative HPLC, **CP 5** was obtained at >95% purity at an overall yield of 53% for the six-step solid phase peptide synthesis. The purified **CP 5** (molecular mass is 371 g/mol) was characterized by electrospray ionization (ESI) mass spectrometry (MS). The observed mass for the $[M+H]^+$ ion corresponds to the calculated value of 372.

2.3. Isothermal titration calorimetry

Microcalorimetric titrations of peptides with metal ions were conducted by isothermal titration microcalorimetry (ITC) using a Microcal VP-ITC Instrument (Northampton, Massachusetts, USA). Pulse calibration (or *Y*-axis calibration) is achieved by dissipating a known power through a resistive heater located on the cell wall and then adjusting the software coefficient for Differential Power (DP). The ITC temperature calibration is conducted with two capillary temperature standards (Octadecane, m.p. 28.2 °C, and *n*-Hexatriacontane, m.p. 75.9 °C). The measured transition midpoints are maintained within ±0.2° of the know transition points (28.2 °C, 75.9 °C) by adjusting the temperature calibration coefficients if necessary. Experiments were carried out at 30 °C in degassed 30 mM MOPS at pH 7.4. Peptide concentrations ranged from 0.075 to 0.15 mM (1.34 mL sample cell), while the metal ion concentrations varied from 1.5 to 3.0 mM in the syringe. These solutions were degassed for 5 min by using the Microcal Thermo Vac degassing unit, and then stored under nitrogen to minimize sample oxidation. After degassing, the VP-ITC auto-pipette was filled with the mercury(II) solution and purged three times to dislodge any bubbles formed in the injection syringe. The degassed peptide solution was loaded into the calorimetric sample cell using a 2.5 mL syringe [20]. Automated titrations of mercury(II), at 6 μL per injection with a duration of 12 s, were conducted until saturation, up to a mercury(II)/peptide mole ratio of about 3.5. Each experiment was repeated at least three times. Heats of dilution and mixing for each experiment were measured by titrating the mercury(II) solution into 30 mM MOPS at pH 7.4. The effective heat of each peptide metal ion interaction was corrected for dilution and mixing effects by subtracting the enthalpy change derived from the titration of mercury(II) in buffer solution into the buffer solution without the peptide.

The heats of bimolecular interactions were obtained by integrating the peak following each injection of metal ion. The binding isotherms were derived from the raw ITC data following correction for dilution and mixing effects. These isotherms were fitted using the two-site model by a nonlinear least square analysis [21,22] with Microcal Origin 7.0 software (Microcal Sofware, Inc., Northampton, Massachusetts, USA) to determine the molar enthalpy change for binding, ΔH, and the corresponding binding constant, K_b. From these values, the thermodynamic characterization of the interaction at experimental temperature can be determined from the fundamental equations of thermodynamics, $\Delta G = -RT\ \ln K_b$ and $\Delta S = (\Delta H - \Delta G)/T$.

At least three separate experiments were conducted for each compound (**CP 1–5**) and the results were used to calculate the mean values of ΔH, K_b, and ΔS. The standard error mean values were calculated for ΔH, K_b, and ΔS based on the variation of such values from at least three separate experiments. Individual ΔG values were calculated from each experimental data set by using the equation $\Delta G = \Delta H - T\Delta S$, and they provided the basis for the calculation of the mean and standard error mean values.

The binding constant, K_b, between mercury(II) ions and peptide is represented by Eq. (1) [21]. The relationship between bulk and free mercury(II) concentrations (L_t and L) in the sample cell volume is given by Eq. (2).

$$K_1 = \frac{[\text{bound Hg}]}{[\text{free binding site 1}][\text{free Hg}]} = \frac{\Theta_1}{(1-\Theta_1)[L]} \text{ and}$$

$$K_2 = \frac{[\text{bound Hg}]}{[\text{free binding site 2}][\text{free Hg}]} = \frac{\Theta_2}{(1-\Theta_2)[L]} \text{ and} \quad (1)$$

$$[L_t] = [L] + [M_t](n_1\Theta_1 + n_2\Theta_2) \quad (2)$$

where $\Theta_m = [\text{bound Hg}]/n_m[M_t]$ is the fraction of peptide binding sites occupied by Hg, $[M_t]$ is the total peptide molar concentration, and n the number of binding sites for Hg (the number of moles of Hg bound to each mole of peptide at saturation of the binding sites). Solving Eq. (1) for Θ_1 and Θ_2, and then substituting into Eq. (2), gives the following equation:

$$[L_t] = [L] + \frac{n_1[M_t][L]K_1}{1+[L]K_1} + \frac{n_2[M_t][L]K_2}{1+[L]K_2} \quad (3)$$

where K_1 and K_2 are the first and second binding constants, respectively. Clearing Eq. (3) of fractions and collecting like terms leads to a cubic equation of the form as shown in the following equation:

$$[L]^3 + p[L]^2 + q[L] + r = 0 \quad (4)$$

where

$$p = \frac{1}{K_1} + \frac{1}{K_2}(n_1+n_2)[M_t] - [L_t]$$

$$q = \left(\frac{n_1}{K_2} + \frac{n_2}{K_1}\right)[M_t] - \left(\frac{1}{K_1} + \frac{1}{K_2}\right)[L_t] + \frac{1}{K_1K_2}$$

$$r = \frac{-[L_t]}{K_1K_2} \quad (5)$$

Eqs. (4) and (5) are then solved for $[L]$, the free Hg concentration, by using MicroCal Origin® 7 program. Both Θ_1 and Θ_2 are then obtained from Eq. (1). The total heat constant Q of the solution in the sample cell of volume V_0 at fractional saturation is,

$$Q = [M_t]V_0(n_1\Theta_1\Delta H_1 + n_2\Theta_2\Delta H_2) \quad (6)$$

where ΔH is the enthalpy of binding per mole of bound Hg. After a correction for displaced volume, and that the instrument senses the change of heat content at the ith injection, ΔQ_i, the pertinent calculated heat effect for the ith injection is

$$\Delta Q_i = Q_i + \frac{dV_i}{V_0}\left[\frac{Q_i + Q_{(i-1)}}{2}\right] - Q_{(i-1)} \quad (7)$$

where ΔV_i is the injection volume at the ith injection. The above equations are simultaneously fitted to the experimental values of ΔQ_i in the Marquardt algorithm to obtain best values for the six

Table 1
Thermodynamic parameters of the interactions of Hg(II) with dicysteinyl peptides in 30 mM MOPS buffer at pH 7.4.[a,b,c]

Compounds	K_b (M^{-1})	ΔH (kJ mol^{-1})	ΔG (kJ mol^{-1})	ΔS (J K^{-1} mol^{-1})
CP 1	$(3.3 \pm 0.6) \times 10^9$	−67.4 ± 1.3	−55.2 ± 0.4	−40.6 ± 4.2
	$(6.2 \pm 0.5) \pm 10^5$	−43.9 ± 2.1	−33.5 ± 0.2	−33.9 ± 6.3
CP 2	$(1.3 \pm 0.7) \pm 10^9$	−64.4 ± 7.1	−52.3 ± 1.3	−58.6 ± 3.8
	$(3.5 \pm 0.1) \pm 10^5$	−48.5 ± 1.3	−32.2 ± 0.1	−53.6 ± 3.8
CP 3	$(2.6 \pm 1.0) \pm 10^9$	−67.8 ± 1.3	−54.0 ± 1.7	−46.0 ± 1.7
	$(3.4 \pm 0.2) \pm 10^5$	−45.6 ± 0.1	−32.2 ± 0.2	−44.8 ± 2.5
CP 4	$(1.7 \pm 0.8) \pm 10^9$	−90.4 ± 2.5	−53.1 ± 1.3	−123.4 ± 11.7
	(1.6 ± 0.4) x10^5	−64.4 ± 2.9	−30.1 ± 0.8	−113.8 ± 11.7
CP 5	$(6.6 \pm 1.2) \pm 10^8$	−92.0 ± 0.1	−51.0 ± 0.4	−135.1 ± 2.1
	$(4.9 \pm 1.0) \pm 10^5$	−68.6 ± 0.8	−33.1 ± 0.4	−118.4 ± 4.2

[a] Values correspond to the mean of three experiments and the mean standard error.
[b] Mercury(II) nitrates.
[c] Detection limits of ITC ($10^2 < K_b < 10^{10}$ M^{-1}).

fitting parameters until no further improvements in the fit occurs with additional iterations [21].

2.4. LTQ Orbitrap mass spectrometry

Samples were analyzed on a hybrid linear ion trap – orbitrap instrument, the LTQ–Orbitrap (Thermo Fisher, San Jose, CA). ESI-MS spectra were acquired in positive ion mode. The solvent was a mixture of 10% acetonitrile in 5 mM ammonium formate buffer at pH 7.5. Direct sample injections (10–50 μL) were carried out at a flow rate of 10 μL/min with a source temperature of 275 °C. The applied spray voltage was 4000 V, the sheath liquid flow was 11 (arbitrary units) without auxiliary gas, and the tube lens voltage was in the range of 90–130 V. The capillary voltage was varied in the range of 20–50 V. The tube lens voltage and the capillary voltage were tuned for every peptide; the applied voltages were directly proportional to the molecular weight of the peptide. Mass

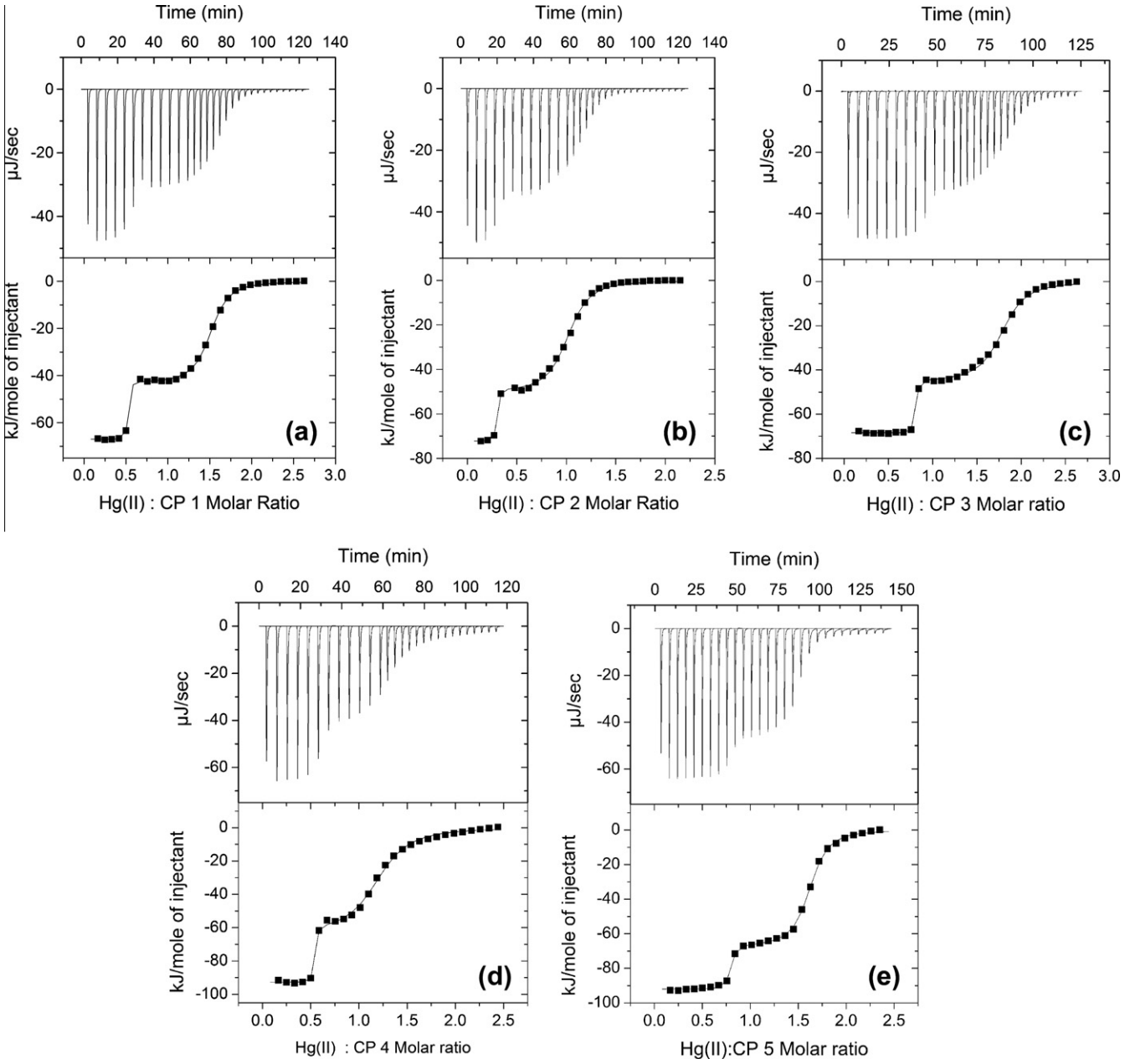

Fig. 2. ITC data curve of (a) **CP 1**, (b) **CP 2**, (c) **CP 3**, (d) **CP 4**, and (e) **CP 5** following titration with Hg(II). Raw ITC titration data (top panels). Binding isotherms (bottom panels) are derived from the data in the corresponding top panels following correction for dilution and mixing effects.

spectra were acquired in the Orbitrap analyzer with a resolution of $R = 60{,}000$. Freshly prepared samples containing different molar ratios of Hg(II) and peptides (Hg(II): peptide ratios of 1:2, 1:1, and 1:0.5), were prepared in degassed, buffered medium (5 mM ammonium formate, pH 7.5) and analyzed promptly to minimize oxidation. The peptide stock solutions and reaction mixtures were prepared fresh daily with degassed solutions using ultrasonication (2×5 min) followed by nitrogen purging. The concentration of Hg(II) was fixed at 7.5×10^{-6} M. MS scans were acquired over an m/z range of 200–2000.

3. Results and discussion

The binding affinity values of dicysteinyl peptides (**CP 1**–**5**) for mercury(II), and their associated thermodynamic parameters are summarized in Table 1. Fig. 2 shows the total measured heat associated with each titration of mercury(II), and the binding isotherms derived from the heat change following each titration of mercury(II) into **CP 1–5** following corrections for dilution and mixing effects. As previously reported for some thiol S-donor peptides [19,23], these cysteinyl peptides show two exothermic interactions following titrations with mercury(II).

A strong exothermic association takes place at the beginning of each titration of mercury(II) into the dicysteinyl peptides (**CP 1–5**) (Fig. 2a–e). This could be attributed to the formation of Hg–S coordinate bond(s) associated with very strong formation constants. As shown in Fig. 2a–e, the curve fitting for this very tight first binding is limited to two data points in most cases; therefore, formation constants are estimated for these compounds as shown in Table 1 (10^8–10^9 M^{-1}). Soft donor and soft acceptor interactions are usually strongly exothermic. At the beginning of the titration, the relative concentration of dicysteinyl peptides is higher than that of mercury(II). Therefore, it is likely that two dicysteinyl peptide molecules bind one mercury(II) ion to form a two-coordinate complex corresponding to a Hg(**CP**)$_2$ complex [Hg(II):**CP** molar ratio of 1:2]. This would be consistent with the coordination chemistry of mercury(II) (d^{10}), a soft acid that has a tendency to form linear thiolate complexes with a coordination number of 2 [18]. Alternatively, two dicysteinyl peptides might bind mercury(II) ion to form a three- or four-coordinate complex. Although the free energies associated with the first complex formations are not significantly different (Table 1, ΔG_1 values range from -51 to -55 kJ mol^{-1}), the enthalpy change values for complex formation between **CP 4** and **CP 5** with mercury(II) (average $\Delta H_1 \sim -91$ kJ mol^{-1}) are about one and a half times larger than the related values for **CP 1**, **2** and **3** (average $\Delta H_1 \sim -66$ kJ mol^{-1}). Correspondingly, the associated entropy change for these structurally larger dicysteinyl peptides (**CP 4** and **5**) (average values of $\Delta S_1 \sim -129$ J K^{-1} mol^{-1}) is less favorable compared to **CP 1**, **2**, and **3** (average values of $\Delta S_1 \sim -48$ J K^{-1} mol^{-1}), which would be in agreement with a more ordered and structurally compact complex.

The second complex formation constant for these dicysteinyl compounds (**CP 1–5**) with mercury (II) (K_2 values range from 1.6×10^5 to 6.2×10^5 M^{-1}) are shown in Table 1. These association constants are in excess of a thousand times weaker than their corresponding first association constants (K_1 values range from 6.6×10^8 to 3.3×10^9 M^{-1}). Their associated free energy change (Table 1, ΔG_2 values range from -30.1 to -33.5 kJ mol^{-1}) are approximately a third less than that observed for the first complex formation (ΔG_1 values range from -51.0 to -55.2 kJ mol^{-1}).

The ΔH_2 and ΔS_2 trends for the formation of the second mercury(II)–peptide complexes are similar to that observed for the formation of the first. The ΔH_2 values for the structurally larger complexes (average $\Delta H_2 \sim -66$ kJ mol^{-1}) formed by **CP 4** and **5** are approximately one and a half times larger than the smaller complexes formed by **CP 1**, **2**, and **3** (average $\Delta H_2 \sim -46$ kJ mol^{-1}).

Table 2
Mercury–peptide complexes signals in the LTQ/Orbitrap MS spectra in ammonium formate buffer at pH 7.5.

Cysteinyl tripeptides	Hg(II):peptide molar ratio in mixture[a]	Peptide molecular ion $(M+H)^+$ (m/z)	Complex ions (m/z) (Hg:peptide stoichiometry)
CP 1		282.0589	
	1:2		482.0139 (1:1) major
			761.0607 (1:2)
	1:1		482.0141 (1:1)
	1:0.5		482.0139 (1:1)
CP 2		296.1667	
	1:2		496.0290 (1:1) major
			789.0931 (1:2)
	1:1		496.1667 (1:1)
	1:0.5		496.0286 (1:1)
CP 3		310.0905	
	1:2		510.0465 (1:1), major
			819.1301 (1:2)
	1:1		510.0833 (1:1)
	1:0.5		510.2500 (1:1)
CP 4		324.1052	
	1:2		524.0605 (1:1), major
			845.1427 (1:2)
	1:1		524.0623 (1:1)
	1:0.5		524.0600 (1:1)
CP 5		372.1064	
	1:2		572.0622 (1:1), major
			943.1622 (1:2)
	1:1		572.0622 (1:1), major
			943.1631 (1:2)
			1140.1158 (2:2)
	1:0.5		572.0622 (1:1), major
			1140.1151 (2:2)

[a] The concentration of Hg(II) in the sample mixture is fixed at 7.5×10^{-6} M.

Their associated ΔS_2 values (~ -116 J K^{-1} mol^{-1}) are less thermodynamically favorable compared to **CP 1**, **2**, and **3** (average values of $\Delta S_2 \sim -44$ J K^{-1} mol^{-1}). The above thermodynamic trends indicate that the larger dicysteinyl peptides (**CP 4** and **5**) could potentially form relatively higher ordered complex structures than CP **1–3**. However, their larger unfavorable entropy changes may also be associated with conformational changes or 'rigid body' interactions during the associations. Conformational changes are entropically unfavorable, and 'rigid body' interactions may also incur an entropic penalty [24,25].

In the monocysteinyl peptides, as previously reported [19], the mercury–peptide formation constants decrease as the size increases from a di- to a tri-peptide due to a smaller contribution from the enthalpy term. Remarkably, in the present series of dicysteinyl tripeptides, the enthalpy change is larger for the structurally larger **CP 4** and **5** than for **CP 1–3**. These dicysteinyl peptides exhibit free energies of complexation that are largely driven by a favorable enthalpy term wherein their $\Delta H/\Delta S$ data pairs fall in the negative ΔH and negative ΔS quadrant of the ΔH versus ΔS plot [19]. The thermodynamic signatures for the dicysteinyl peptides are clearly different from the monocysteinyl peptides. We postulate that the enhanced stability of complexes containing chelate rings or two ligating groups per molecule (dicysteinyl peptides) contributes to this difference. Although the chelate effect is chiefly an entropy effect, often additional stabilization results from enthalpy changes [15b]. Given the complexity of the thermodynamics associated with chelation, other factors which are not apparent, may also contribute to the above thermodynamic differences for complex formations between the monocysteinyl and dicysteinyl peptides with mercury(II).

It is also noteworthy that the stability constants for the mercury(II)–cysteinyl peptide complexes, as determined by ITC in

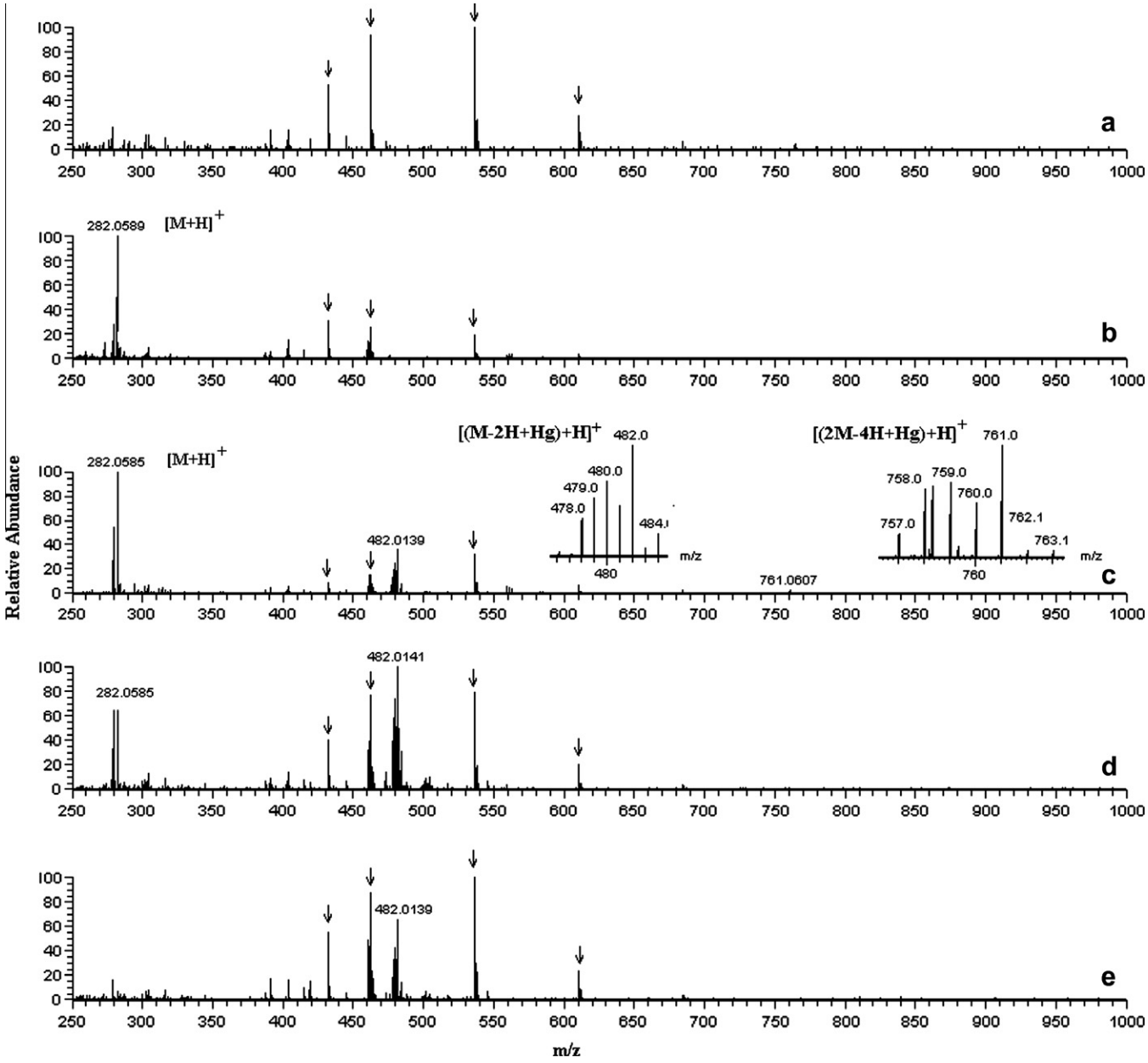

Fig. 3. Electrospray ionization orbitrap mass spectra from a solution containing (a) 5 mM ammonium formate buffer at pH 7.5. Some common low molecular mass contaminants detected for leached substances (peaks with m/z values at 432, 460, 536 and 610) are indicated by arrows. (b) 7.5×10^{-6} M **CP 1** in ammonium formate buffer, (c) 7.5×10^{-6} M Hg(II) and 1.5×10^{-5} M **CP 1** (1:2 ratio), (d) 7.5×10^{-6} M Hg(II) and 7.5×10^{-6} M **CP 1** (1:1 ratio), and (e) 7.5×10^{-6} M Hg(II) and 3.75×10^{-6} M **CP 1** (1:0.5 ratio). Insets show the mercury isotopic signatures of the Hg(peptide) and Hg(peptide)$_2$ complexes detected.

MOPS buffer, pH 7.4, are lower than reported values for mercury(II)–cysteine or mercury(II)–glutathione by polarographic [26] or potentiometric methods [27]. ITC measures the enthalpy change for a bimolecular binding interaction at a constant temperature and pH. However, enthalpy values are dependent on buffer, pH, and temperature. With regard to buffer, the enthalpy effect is primarily due to the fact that the heat of ionization is different for each buffer type. Additionally, if there is a change in protonation during binding, the enthalpy value will vary in different buffer systems. This is also called proton linkage [28]. Consequently, the energetics of Ca(II)–EDTA interactions as studied by ITC have been reported to be dependent on buffer type. Griko [29] reported that the equilibrium binding constant (K_b) for Ca(II)–EDTA is highly dependent on buffer type, which can result in a dramatic decrease in Ca(II) affinity due to the reduction of the enthalpy term of the stability constant. Wilcox [30] showed that there are two necessary considerations to reproduce literature binding constants by ITC. First, the true pH-dependent binding constants and second, the metal ion interaction with buffer must be determined. In this study, both these considerations are independent variables because the experiments were conducted in the same buffer system involving similar bimolecular interactions (thiols and mercury(II)).

The ΔH values for the formation of Hg–S bonds between methylmercury(II) and cysteinate in 0.15 M sodium perchlorate in water at 25 °C has been reported to be -76.2 ± 6 kJ mol^{-1} [31]. The stability constant of the CH_3Hg(cysteinate) complex is 3.98×10^{16} M^{-1}, which is largely contributed by favorable enthalpy and entropy terms. In comparison, the enthalpy values for complex formation between **CP 1**, **2** and **3** with mercury(II) nitrate at pH 7.4 in 30 mM MOPS at 30 °C are $\Delta H_1 \sim -66$ kJ mol^{-1} and $\Delta H_2 \sim -46$ kJ mol^{-1}.

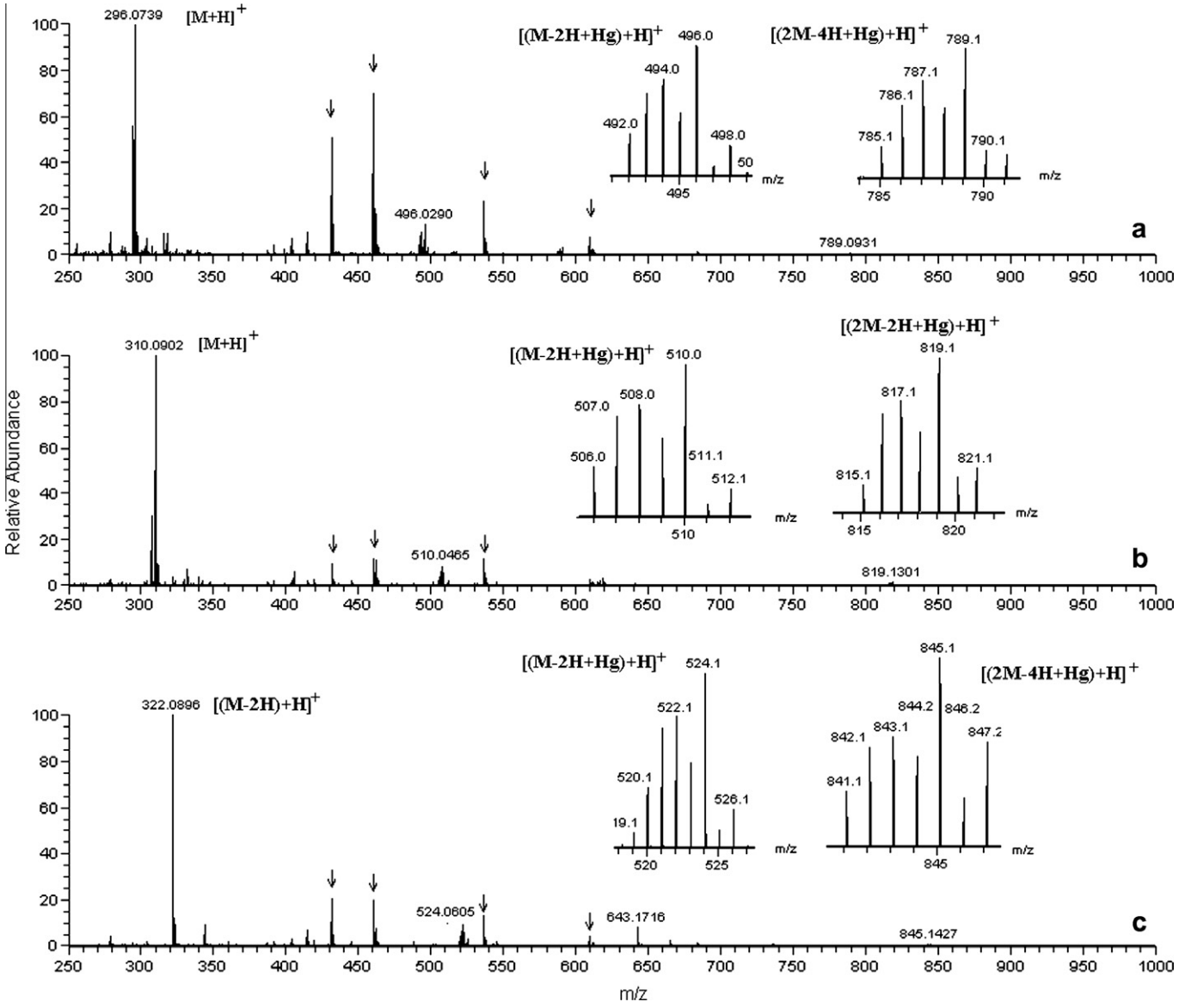

Fig. 4. Electrospray ionization orbitrap mass spectra from a solution containing (a) 7.5×10^{-6} M Hg(II) and 1.5×10^{-5} M (1:2 ratio) of (a) **CP 2**, (b) **CP 3**, and (d) **CP 4**. Insets show the mercury isotopic signatures of the Hg(peptide) and Hg(peptide)$_2$ complexes detected.

The corresponding values for **CP 4** and **5** are $\Delta H_1 \sim -91$ kJ mol^{-1} and $\Delta H_2 \sim -66$ kJ mol^{-1} (Table 1). However, the stability constant for the formation of these complexes are entropically disfavored (negative ΔS values) (Table 1). This unfavorable entropy term coupled with the proton linkage effect could likely constitute the observed relatively lower stability constants derived from binding enthalpy.

For the above reasons, the ITC derived formation constant values from binding enthalpy values could be expected to be different from stability constants derived with other methods that are based on the determination of concentration of species. The purpose of this study is to investigate the effects of increasing the distance between cysteinyl residues of tripeptides on their mercury(II) associations. The comparison of the relative thermodynamic values associated with mercury(II) and cysteinyl peptides interactions by ITC are meaningful because this comparative study is conducted in the same buffer system and with similar analogues of dicysteinyl tripeptides.

The ITC data for **CP 1–5** (Fig. 2a–e) showed variations in Hg:**CP** ratio (0.5 ± 0.25) at which the first measured enthalpy changes following titration with mercury(II). This variation could be in part due to the hydroscopic nature of these peptides, which contributed to experimental errors associated with determination of the amount of peptide. Additionally, any deviations in the purity of the mercury(II) solution could also constitute variations in the above ratio. Based on the observed variations in Hg:CP ratios, the stoichiometry of the complexes formed during the sequential titration of mercury(II) into the peptide solution could not be readily confirmed. In order to characterize the possible complex composition for **CP 1–5** and mercury (II), we subsequently conducted electrospray ionization orbitrap mass spectrometry (ESI-MS) studies. Reaction mixtures of mercury(II) nitrate and peptide were prepared in a volatile buffer, ammonium formate, and the resulting reaction complexes were analyzed with electrospray ionization orbitrap mass spectrometry (ESI-MS). The soft energies employed in ESI-MS do not significantly fragment metal ion and peptide complexes and consequently offer a means of obtaining the stoichiometries of mercury(II)–cysteinyl peptide complexes [32–34]. Additionally the presence of the seven stable isotopes of mercury (with ^{202}Hg being the most abundant at 29.86%) as components of peptide complexes

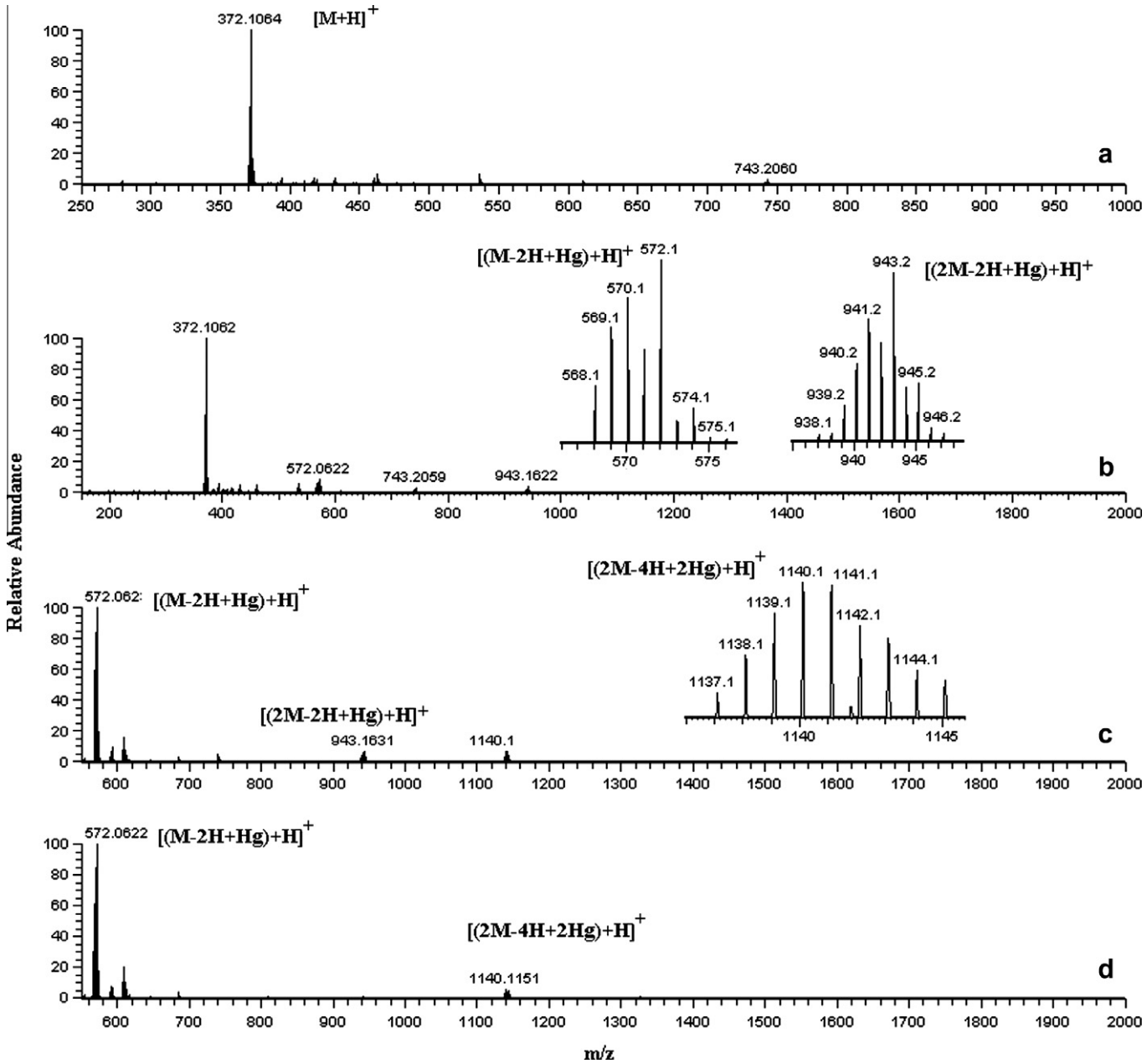

Fig. 5. Electrospray orbitrap mass spectra from a solution containing (a) 7.5×10^{-6} M **CP 5**, (b) 7.5×10^{-6} M Hg(II) and 1.5×10^{-5} M **CP 5** (1:2 ratio), (c) 7.5×10^{-6} M Hg(II) and 7.5×10^{-6} M **CP 5** (1:1 ratio), and (d) 7.5×10^{-6} M Hg(II) and 3.75×10^{-6} M **CP 5** (1:0.5 ratio). Insets show the mercury isotopic signatures of the Hg(peptide), $Hg(peptide)_2$, and $Hg_2(peptide)_2$ complexes detected.

will yield distinct isotope distribution patterns that can provide further evidence for the number of mercury ions binding to the cysteinyl peptides [35]. Although ESI-MS offers a powerful means of characterizing these complexes, it should be emphasized that the experimental conditions under which these complexes form differ from those employed in the isothermal titration calorimetry experiments. For example, ESI-MS necessitates the use of a volatile buffer system, which precludes the use of MOPS as the buffering medium. Additionally, a significantly more dilute reaction mixture is preferable for ESI-MS analysis to minimize mercuric residues in the MS system. Consequently, the complexes observed by ESI-MS may not entirely reflect the exact complexes present in the ITC experiments. However, ESI-MS will provide a sampling of some definitive mercuriated peptide adducts that are formed under the specified electrospray ionization conditions.

Complexation of mercury(II) with **CP 1**–**5** was investigated by reacting mixtures of mercury(II) and peptide at three different molar ratios (mercury(II): peptide ratios of 1:2, 1:1, and 1:0.5), where the concentration of mercury(II) is 7.5×10^{-6} M and the peptide concentration is varied accordingly. Table 2 shows a summary of the observed signals for the complexes formed as *m*/*z* values. In general, these dicysteinyl peptides formed two types of complexes corresponding to $Hg(peptide)_2$ (minor) and Hg(peptide) (major) when the reaction mixtures contain excess peptide. However, in equimolar mixtures of the reacting species or in excess mercury(II), a 1:1 interaction predominates to form only the Hg(peptide) complex. On the other hand, **CP 5** formed a third type of complex corresponding to $Hg_2(peptide)_2$. This could be attributed to the conformationally less flexible aryl linker between the cysteinyl residues in **CP 5**.

The ESI mass spectrum for **CP 1** shows the molecular ion peak [**CP 1**+H]$^+$ (m/z = 282) (Fig. 3). Some common low molecular mass contaminants detected for common leached substances from plastic tubing (peaks with m/z values at 432, 460, 536 and 610) are also observed and are indicated by arrows in Fig. 3a. The addition of mercury(II) to **CP 1** (1:2 M ratio) produced a mass spectrum with a base peak corresponding to the molecular ion [**CP 1**+H]$^+$ (m/z = 282), and weak peaks corresponding to the adduct for two types of complexes, Hg(peptide)$_2$ [(2**CP 1**–4H+Hg)+H]$^+$ (m/z = 761), and Hg(peptide) [(**CP 1**–2H+Hg)+H]$^+$ (m/z = 482) (Fig. 3c). Fig. 3c insets show the mercury isotopic signature in the peptide–mercury adducts. Mercury has seven main naturally occurring isotopes: ^{196}Hg, ^{198}Hg, ^{199}Hg, ^{200}Hg, ^{201}Hg, ^{202}Hg, ^{204}Hg, with percent natural abundances of 0.146%, 10.02%, 16.84%, 23.13%, 13.22%, 29.80%, and 6.85%, respectively. The two major isotopes ^{200}Hg and ^{202}Hg show a distinct relative intensity ratio of 2.3:3. The observed isotope cluster for these complexes (Fig. 3c) matches well with the mercury signature pattern, which provides further evidence for the presence of one mercury ion binding to the dicysteinyl peptide(s). Based on the above premises, we postulate that mercury forms a two-coordinate complex in the Hg(**CP 1**) adduct. The monoisotopic mass for the Hg(**CP 1**) adduct (m/z = 482) correlates well with a two-coordinate complex, which would require the deprotonation of two cysteinyl thiols to form the [(**CP 1**–2H+Hg)+H]$^+$ adduct. On the other hand, the monoisotopic mass for the Hg(**CP 1**)$_2$ adduct (m/z = 761) requires deprotonation of four cysteinyl thiols to form the [(2**CP 1**–4H+Hg)+H]$^+$ adduct. Based on the number of deprotonations observed for this adduct, mercury could form a four-coordinate complex with the four thiolates, or it could form a two-coordinate complex with two cysteinyl thiolates whereas the remaining two cysteinyl residues form cystine. In solutions containing molar ratios of mercury(II) to **CP 1** of 1:1 or 1:0.5, the only cationic adduct detected corresponded to the Hg(peptide) complex (Fig. 3d and e).

Similar types of Hg(peptide)$_2$ and Hg(peptide) complexes were observed for **CP 2** as shown in Fig. 4a. Fig. 4a insets show the general mercury isotopic signature in the **CP 2**-mercury adduct clusters as previously described for **CP 1**. Two types of mercury–peptide complexes were also observed for each of **CP 3** and **CP 4**. The monoisotopic mass for the Hg(**CP 3**) adduct (m/z = 510) and the Hg(**CP 4**) adduct (m/z = 524) corresponds to the formation of the [(peptide–2H+Hg)+H]$^+$ adduct. This correlates with the probable formation of a two-coordinate complex as observed for Hg(**CP 1**), which would require the deprotonation of two cysteinyl thiols. The Hg(**CP 3**)$_2$ complex corresponds to a [(2**CP 3**–2H+Hg)+H]$^+$ adduct (m/z = 819, Fig. 4b), which matches with mercury forming coordinate bonds with two cysteinyl thiolates; the remaining two cysteinyl residues in the complex exist as thiols. However, the Hg(**CP 4**)$_2$ complex corresponds to a [(2**CP 4**–4H+Hg)+H]$^+$ adduct (m/z = 845, Fig. 4c). The monoisoptopic mass for this mercury–complex ion adduct is indicative of the formation of a two- or four-coordinated complex as exhibited by Hg(**CP 1**)$_2$ and Hg(**CP 2**)$_2$.

From the above ESI-MS data, we postulate that mercury forms a two-coordinate Hg(CP) complex, and it forms either a two- or four-coordinate Hg(CP)$_2$ complex with **CP 1, 2 3,** and **4** in ammonium formate buffered solutions. In reaction mixtures containing an equivalent amount of mercury(II) and peptide, or in excess mercury(II), the only cationic complex adduct detected corresponded to the Hg(CP) type complex (Table 2).

Fig. 5 shows that the aryl dicysteinyl peptide (**CP 5**) formed a similar two-coordinate Hg(**CP 5**) complex as observed for **CP 1–4**. However, its protonated monoisotopic peak for the Hg(**CP 5**)$_2$ adduct (m/z = 943) (Fig. 5b) correlates with the formation of two coordinate bonds with cysteinyl thiolates (Fig. 6a), which requires deprotonation of two cysteinyl thiols to form the [(2**CP 5**–2H+Hg)+H]$^+$ adduct. This could be attributed to the conformationally less flexible aryl linker between the cysteinyl residues in

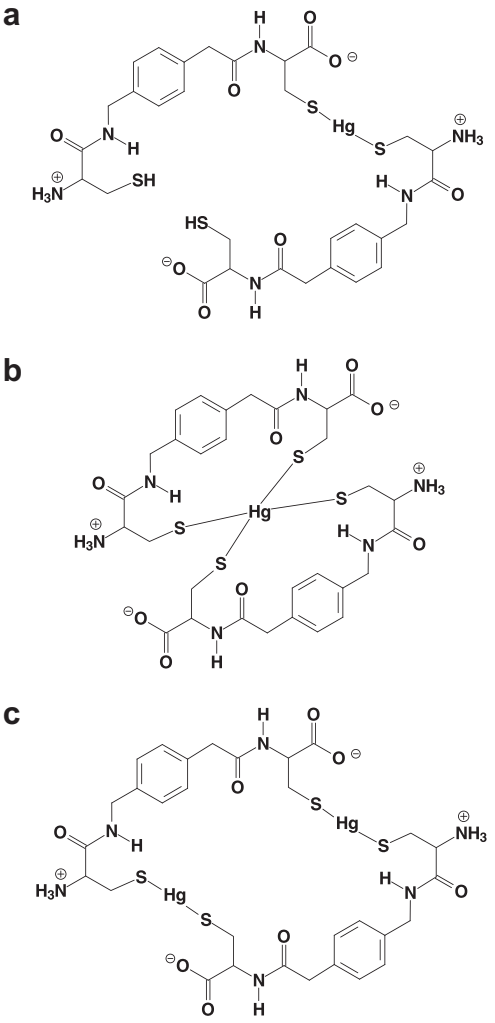

Fig. 6. Chemical structures of (a) a two coordinate complex which requires deprotonation of two cysteinyl thiols to form the [(2**CP 5**–2H+Hg)+H]$^+$ adduct, (b) a four coordinate complex which requires deprotonation of four cysteinyl thiols to form the [(2**CP 5**–4H+Hg)+H]$^+$ adduct, and (c) a dual two coordinate complex corresponding to the Hg$_2$(peptide)$_2$ complex.

CP 5 which prevents the formation of the four-coordinate complex (Fig. 6b) involving four cysteinyl thiolate groups. Remarkably, **CP 5** formed a third type of complex corresponding to a two-to-two Hg$_2$(peptide)$_2$ complex (Fig. 6c). Fig. 5c inset shows the isotopic cluster for this Hg$_2$(peptide)$_2$ complex. It matches well with the theoretical isotopic patterns for [(2**CP 5**–4H+2Hg)] ($C_{30}H_{38}Hg_2N_6O_8S_4$). Calculations conducted with the ChemCalc program [36] yielded a monoisotopic mass corresponding to an m/z value of 1142. Fig. 5c inset shows the two-mercury isotopic signature for the protonated adduct [(2**CP 5**–4H+2Hg)+H]$^+$, and the corresponding protonated monoisotopic mass (m/z = 1143), which is quantitatively three mass units larger than the m/z value of the most intense peak in the isotope cluster. This is in agreement with the monoisotopic peak position in the calculated isotopic pattern [35].

In summary, the above results show that peptides containing *N*- and *C*-terminal cysteinyl residues (**CP 1–5**) can serve as effective ligating groups or "anchors" to accommodate the coordination sites of mercury(II). Based on the ESI-MS data, it is also evident that the type of mercury–peptide complex formed depends on the initial ratio of mercury(II):peptide. In the Hg(peptide)$_2$ complex type, **CP 1–4** form two- or four-coordinated complexes with mercury(II) whereas **CP 5** forms a two-coordinate complex due to its less

flexible tethering aryl linkage between the two cysteinyl residues. The formation constants for the Hg(peptide)$_2$ complexes are more than a thousand fold higher than for the corresponding Hg(peptide) complexes.

4. Conclusion

By using calorimetry, we have gained more insight into the associations of mercury(II) with dicysteinyl tripeptides in MOPS buffered solutions at pH 7.4. ESI mass spectrometry also afforded a reliable determination of the content of complexes, which showed that the type of mercury–peptide complex that is present depends on the initial ratio of mercury(II):peptide. Although ESI mass spectrometry data provided an accurate stoichiometry of mercury and peptide in the complexes formed, it is necessary to use additional methods (for example, ^{1}H, ^{13}C, ^{199}Hg NMR spectroscopy or potentiometry) in order to detect the content of complexes in solution. In summary, we found that *n*-alkyl dicysteinyl peptides (**CTP 1–4**) and the aryl dicysteinyl peptide (**CTP 5**) can serve as effective "double anchors" to accommodate the coordination sites of mercury(II) to form Hg(peptide) complexes. However, the distance between these cysteinyl residues does not significantly affect their binding affinity for mercury(II). In general these interactions result in a decrease in entropy, indicating that these mercury–peptide complexes form highly ordered structures.

Finally, the strong mercury(II) binding affinity and the efficient complex formation assumed by these dicysteinyl peptides make them striking molecular templates for additional design expectations. For example, the formation constants for the Hg(peptide)$_2$ complexes (two- or four-coordinate complexes) are significantly higher than the corresponding Hg(peptide) complexes (two-coordinate complexes). Therefore, tethering two dicysteinyl peptides to form a single peptide chain consisting of four cysteinyl groups could enhance binding affinity for mercury(II) by its propensity to form a four-coordinate complex of the type Hg(peptide), which could be thermodynamically more favorable through chelation effects. Moreover, the dicysteinyl tripeptide (Cys-Trp-Cys) from our previous study [19] formed a complex with mercury, which exhibited a higher stability constant than the current dicysteinyl tripeptide (Cys-Gly-Cys). Therefore, it is anticipated that adding auxiliary binding group(s) between the two cysteinyl groups could significantly enhance the stability constant of some mercury–dicysteinyl tripeptide complexes. We are currently studying the effect of varying the amino acid sequence of some tri- and tetra-cysteinyl peptides to evaluate the effect of auxiliary ligating groups on mercury binding. These multi-cysteinyl peptides could also be more efficient in binding more than one mercury ion per peptide molecule. Additionally, they would form structurally larger molecular complexes, which could better evade transport into brain cells via amino acid transporters by molecular mimicry [16,17].

We are also working toward the elucidation of probable mercury(II) and peptide complex structures by performing density functional theory calculations on a variety of possible structures. These studies will provide structural information for designing optimal cysteinyl peptide structures as effective chelators of mercury(II).

Acknowledgments

M.N.-S. acknowledges support from the National Science Foundation, RUI Grant CHE 1011859, and the National Institute of Health, NIGMS SC3 Grant SC3GM088134. J.B. and M.B. acknowledge support from the NSF HBCU-Undergraduate Program. The authors thank C.L. Colyer (Wake Forest University) and V. Frasca (MicroCal Inc., GE Healthcare) for helpful suggestions and comments regarding this work.

References

[1] F.A. Cotton, G. Wilkinson, C.A. Murillo, M. Bochmann, Advanced Inorganic Chemistry, sixth ed. John Wiley and Sons, Inc., New York, 1999, pp. 590–629 (Chapter 15).
[2] U.S. Environmental Protection Agency. <http://www.epa.gov/mercury/control_emissions/global.htm> (accessed on 01.06.12).
[3] World Health Organization, Exposure to Mercury: A Major Health Concern. Geniva, World Health Organization, 2007. <http://www.who.int/phe/news/Mercury-flyer.pdf> (accessed on 01.06.12).
[4] R.K. Zalups, Molecular interactions with mercury, Pharmacol. Rev. 52 (2000) 113–143.
[5] O. Andersen, Principles and recent developments in chelation treatment of metal intoxication, Chem. Rev. 99 (1999) 2683–2710.
[6] H.V. Aposhian, R.M. Maiorino, D. Gonzalez-Ramirez, M. Zuniga-Charles, Z. Xu, J.M. Hurlbut, P. Junco-Munoz, R.C. Dart, M.M. Aposhian, Mobilization of heavy metals by newer, therapeutically useful chelating agents, Toxicology 97 (1995) 23–38.
[7] J.R. Campbell, T.W. Clarkson, M.D. Omar, The therapeutic use of 2,3-dimercaptopropane-1-sulfonate in two cases of inorganic mercury poisoning, JAMA 256 (1986) 3127–3130.
[8] W.A. Watson, T.L. Litovitz, W. Klein-Schwartz, G.C. Rodgers Jr., J. Youniss, N. Reid, W.G. Rouse, R.S. Rembert, D. Borys, 2003 annual report of the American association of poison control centers toxic exposure surveillance system, Am. J. Emerg. Med. 22 (5) (2004) 335–404.
[9] J.P.K. Rooney, The role of thiols, dithiols, nutritional factors and interacting ligands in the toxicology of mercury, Toxicology 234 (2007) 145–156.
[10] A. Meister, Glutathione metabolism and its selective modification, J. Biol. Chem. 263 (1988) 17205–17208.
[11] H.J. Church, J.P. Day, R.A. Braithwaite, S.S. Brown, Binding of lead to a metallothionein-like protein in human erythrocytes, J. Inorg. Biochem. 49 (1993) 55–68.
[12] M.H. Zenk, Heavy metal detoxification in higher plants – a review, Gene 179 (1996) 21–30.
[13] R.G. Pearson, Hard and soft acids and bases, Chem. Brit. 3 (1967) 103–107.
[14] F.A. Cotton, G. Wilkinson, C.A. Murillo, M. Bochmann, Advanced Inorganic Chemistry, sixth ed., John Wiley & Sons, Inc., New York, 1999. pp. 615.
[15] (a) J.E. Huheey, E.A. Keiter, R.L. Keiter, Inorganic Chemistry: Principles of Structure and Reactivity, fourth ed., Harper Collins College Publishers, New York, 1993. p. 473;
(b) J.E. Huheey, E.A. Keiter, R.L. Keiter, Inorganic Chemistry: Principles of Structure and Reactivity, fourth ed., Harper Collins College Publishers, New York, 1993. p. 522.
[16] T.W. Clarkson, Molecular and ionic mimicry of toxic metals, Ann. Rev. Pharmacol. Toxicol. 32 (1993) 545–571.
[17] C.C. Bridges, R.K. Zalups, Molecular and ionic mimicry and the transport of toxic metals, Toxicol. Appl. Pharmacol. 204 (2005) 274–308.
[18] C.C. Bridges, C. Bauch, F. Verrey, R.K. Zalups, Mercuric conjugates of cysteine are transported by the amino acid transporter system $b^{0,+}$: implications of molecular mimicry, J. Am. Soc. Nephrol. 15 (2004) 399. 663–673.
[19] M. Ngu-Schwemlein, J. Merle, P. Healy, S. Schwemlein, S. Rhodes, Thermodynamics of the complexation of Hg(II) by cysteinyl peptide ligands using isothermal titration calorimetry, Thermochim. Acta 496 (2009) 129–135.
[20] Microcal LLC, VP-ITC MicroCalorimeter User's Manual, version E-2, 2004, Section 3: Running an ITC Experiment, pp. 36–53.
[21] Microcal LLC, ITC Data Analysis in OriginR, Tutorial Guide version 7, 2004, Lesson 7: Advanced Curve Fitting, 55 and 106.
[22] J.A. Thomson, J.E. Ladbury, in: J.E. Ladbury and M.L. Doyle (Eds.), Biocalorimetry 2: Applications of Biocalorimetry in the Biological Sciences, Wiley, Chichester, 2004, pp. 37–58 (and references within).
[23] M. Ngu-Schwemlein, W. Gilbert, K. Askew, S. Schwemlein, Thermodynamics and fluorescence studies of the interactions of cyclooctapeptides with Hg^{2+}, Pb^{2+}, and Cd^{2+}, Bioorg. Med. Chem. 16 (2008) 5778–5787.
[24] W.H. Ward, G.A. Holdgate, Isothermal titration calorimetry in drug design, Prog. Med. Chem 38 (2001) 309–376.
[25] P. Kwong, M.L. Doyle, D.J. Casper, C. Cicala, S.A. Leavitt, S. Marjeed, T.D. Steenbeke, M. Venturi, I. Chaiken, M. Fung, H. Katinger, P.W. Parren, J. Robinson, D. Van Ryk, L. Wang, D.R. Burton, E. Freire, R. Wyatt, J. Sodroski, W.A. Hendrickson, J. Arthos, Nature 420 (2002) 678–682.
[26] W. Stricks, I.M. Kolthoff, Reactions between mercuric mercury and cysteine and glutathione. Apparent dissociation constants, heats and entropies of formation of various forms of mercuric mercapto-cysteine and -glutathione, J. Am. Chem. Soc. 75 (1953) 5673–5681.
[27] P.D. Oram, X. Fang, Q. Fernando, The formation constants of mercury(II)–glutathione complexes, Chem. Res. Toxicol. 9 (1996) 709–712.
[28] B.M. Baker, K.P. Murphy, Evaluation of linked protonation effects in protein binding reactions, Biophys. J. 71 (1996) 2049–2055.
[29] Y.V. Griko, Energetics of Ca^{2+}–EDTA interactions: calorimetric study, Biophys. Chem. 79 (1999) 117–127.
[30] Y. Zhang, S. Akilesh, D.E. Wilcox, Isothermal titration calorimetry measurements of Ni(II) and Cu(II) binding to His, GlyGlyHis, HisGlyHis, and bovine serum albumin: A critical evaluation, Inorg. Chem. 39 (2000) 3057–3064.
[31] L. Aldeerighi, P. Gans, S. Midollini, A. Vacca, Co-ordination chemistry of the methylmercury(II) ion in aqueous solution: a thermodynamic investigation, Inorg. Chim. Acta 356 (2003) 8–18.

[32] A. D'Agstino, R. Colton, J.C. Traeger, A.J. Canty, An electrospray mass spectrometric study of organomercury(II) and mercuric interactions with peptides involving cysteinyl ligands, Eur. Mass Spectrom. 2 (1990) 273–285.
[33] F.M. Rubino, C. Verduci, R. Giampiccolo, S. Pulvirenti, G. Brambilla, A. Colombi, Molecular characterization of homo- and heterodimeric mercury(II)-bis-thiolates of some biologically relevant thiols by electrospray ionization and triple quadruple tandem mass spectrometry, J. Am. Soc. Mass Spectrom. 15 (2003) 288–300.
[34] E. Chekmeneva, J.M. Diaz-Cruz, C. Arino, M. Esteban, Binding of Hg^{2+} with phytochelatins: study by differential pulse voltametry on rotating Au-disk electrode, electrospray ionization mass spectrometry, and isothermal titration calorimetry, Environ. Sci. Technol. 43 (2009) 7010–7015.
[35] E.M. Krupp, B.F. Milne, A. Mestrot, A.A. Meharg, J. Feldmann, Investigation into mercury bound to biothiols: structural identification using ESI-ion-trap MS and introduction of a method for their HPLC separation with simultaneous detection by ICP-MS and ESI-MS, Anal. Bioanal. Chem. 390 (2008) 1753–1764.
[36] ChemCal: Isotopic Distribution Calculation – Mass Spectra Simulation. <http://www.chemcalc.org> (accessed on 01.03.12).